# 3D NON-AXISYMMETRIC EFFECTS
# IN THE DIII–D BOUNDARY

by
R.A. MOYER AND T.E. EVANS

**GENERAL ATOMICS**

# DISCLAIMER

# 3D NON-AXISYMMETRIC EFFECTS
# IN THE DIII–D BOUNDARY

**by**
**R.A. MOYER AND T.E. EVANS.**

**GENERAL ATOMICS PROJECT 30033
JUNE 2002**

**GENERAL ATOMICS**

# I. INTRODUCTION

3-D effects in tokamaks due to various sources of resonant radial magnetic perturbations $\delta b_r$ include: field errors due to coil misalignments [1]; disruptions and halo currents [2]; and locked modes [3]. Each of these has often been treated as either "fixable" (e.g. coil misalignments) or the result of "off-normal" operation (e.g. disruptions). However, evidence exists that asymmetries affect tokamak operation in "normal" scenarios as well. Toroidally asymmetric divertor heat flux distributions have been reported in both L- and H-mode in ASDEX [4] and DIII-D [5], especially during ELMs and have been correlated with toroidally asymmetric current filaments in the scrape-off layer of DIII-D [5]. Experiments in which external coils are used to create a stochastic boundary have demonstrated that an edge stochastic layer can be used to control power and particle handling at the plasma facing components without degrading core energy confinement [6], and that a stochastic layer can create an H-mode-like radial transport barrier as indicated by the steep electron temperature gradient formed inside the last closed flux surface [7] (see Fig. 6).

## II. SIGNIFICANCE OF 3-D EFFECTS FOR CORE PERFORMANCE

In addition to controlling the plasma interaction with the wall, stochastic boundaries in tokamaks are of interest because of the need for external coils to control locked [3], resistive wall [8], and neoclassical tearing modes [9] in order to achieve high performance. Although designed to control core modes, these coils also perturb the pedestal and scrape-off layer, forming a stochastic layer just inside the unperturbed separatrix. This stochastic layer can impact core performance due to the tight coupling of core transport to pedestal pressure [10]. Because the stochastic layer forms in the pedestal region, resonant magnetic perturbations might be used to control the pedestal height and core performance, as well as the edge stability and ELM behavior; power, particle and helium exhaust; and impurity penetration into the plasma core.

# III.  MODELING THE C-COIL EFFECT

Although there may be other sources of $\delta b_r$ in the DIII-D tokamak, we consider a known source that is well characterized, routinely used, and externally controllable: the C-coil [3]. The C-coil is used to improve core performance by nulling a presumed field error at the $q = 2$ surface in order to reduce locked mode effects and the onset of resistive wall modes. It consists of six midplane saddle loops with opposing coil pairs wired in series with antiparallel phases creating a predominantly $n = 1$ toroidal perturbation spectrum [3]. The C–coil perturbation is modelled with the TRIP3D field line integration code as described in Ref. [11]. The TRIP3D code has been adapted to the DIII–D geometry by using the EFIT Grad-Shafranov plasma equilibrium solver [12] to specify the axisymmetric equilibrium, which is constrained by measured magnetic flux data. This equilibrium contains the full discharge shape with realistic plasma pressure and toroidal plasma current profiles.

## IV. STOCHASTIC LAYERS FORMATION IN AN OHMIC DIVERTOR PLASMA

Because the poloidal mode spectrum contains harmonics $m = 1 - 7$, the C-coil directly perturbs both the core and edge plasma. To illustrate this, we consider a double null diverted Ohmic plasma (Fig. 1). During the first 2500 ms, the C-coil is actively controlled using the standard locked mode feedback algorithm. At 2500 ms the C-coil currents are changed, resulting in a perturbation that doesn't change the profiles at the $q = 2$ surface where locked modes are generally seen. Instead, the edge profiles change consistent with formation of a stochastic boundary with characteristics associated with such layers in non-diverted tokamaks: 1) $T_e$ and $n_e$ profile flattening locally in the edge [Fig. 2(c) and (d)]; 2) increased recycling consistent with connecting field lines from inside the separatrix to the divertor (Fig. 3 inset); and 3) broadened particle flux profile on the divertor floor inferred from broadening of the $D_\alpha$ profile (Fig. 3) [13].
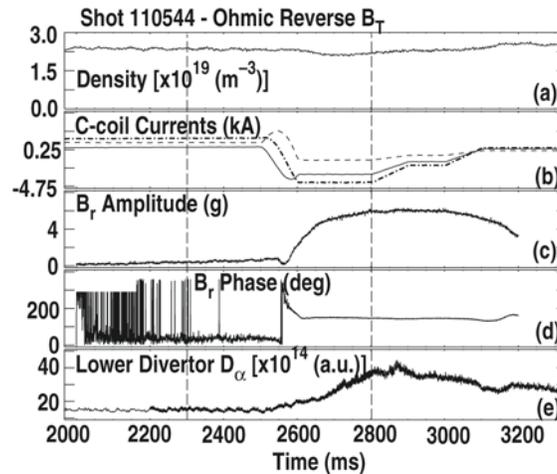


FIG. 1. Plasma response to C-coil change in discharge 110544: (a) line average density, (b) C-coil currents, radial error field (c) amplitude and (d) phase, and (e) divertor $D_\alpha$ recycling near the outer strikepoint.

The TRIP3D code was used to model discharge 110544 at 2800 ms and 2300 ms. At 2800 ms the unperturbed outer separatrix position from EFIT is $r_{sep\_mid\_out} = 0.6349$ m [Fig. 4(a)]. The solid violet line is the DIII-D first wall and the dashed blue line is the unperturbed EFIT separatrix position. The figure shows the field line $r,\theta$ positions after each toroidal transit (black, red and green dots) at a toroidal angle $\phi = 120°$ (the Thomson scattering location: dark blue dots near $\phi = 60°$). The field lines are started at $\phi = 120°$, $\phi = 0$ and $0.5$ m $< r < 0.6349$ m in 0.5 mm steps. The black dots are field lines that do not cross the unperturbed separatrix while the red and green dots are those field lines that cross the separatrix and intersect a material surface. Red field lines are integrated in the forward $B_T$ direction and green lines are integrated in the reverse $B_T$ direction. The modeling shows that the C-coil currents and phases at 2800 ms [Fig. 3(b)] produce a much broader stochastic region than those at 2300 ms. The width of the stochastic region

increases by a factor of 2.5 at the outer midplane between 2300 and 2800 ms, corresponding to 3 and 9 Thomson points at 2300 ms [Fig. 4(a)] and 2800 ms [Fig. 4(b)] respectively, in agreement with the $T_e$ profile changes shown in Fig. 4(c) and 4(d).
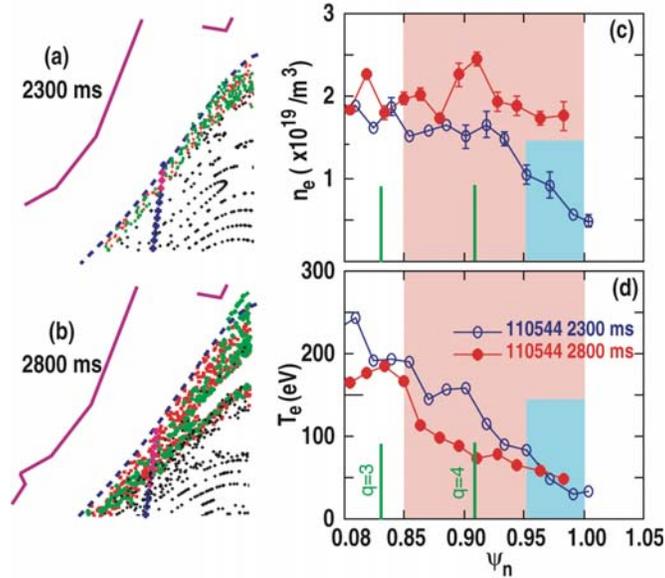


Fig. 2. Expanded view of the field line structure along the Thomson scattering chord at (a) 2300 ms and (b) 2800 ms in discharge 110544. The Thomson scattering points (crosses) are plotted as purple (in) and blue (out) of the stochastic layer. The Thomson (c) density and (d) $T_e$ profiles are plotted at (blue) 2300 ms and (red) 2800 ms. The shaded boxes indicate the predicted extent of the stochastic layer at (light blue) 2300 ms and (light red) 2800 ms. Based on the starting radius of the first field line connecting to a material surface, the width of the stochastic layer is 19 mm (2300 ms) and 44 mm (2800 ms).
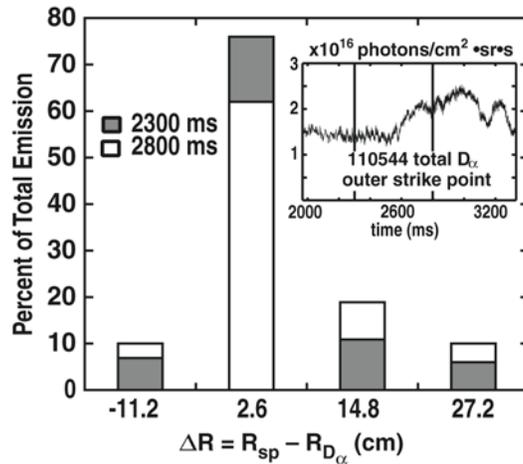


Fig. 3. Broadening of the $D_\alpha$ profile when the stochastic layer is formed. Inset shows the increase in overall recycling. $\Delta R$ is the distance of the $D_\alpha$ measuring chord from the strikepoint
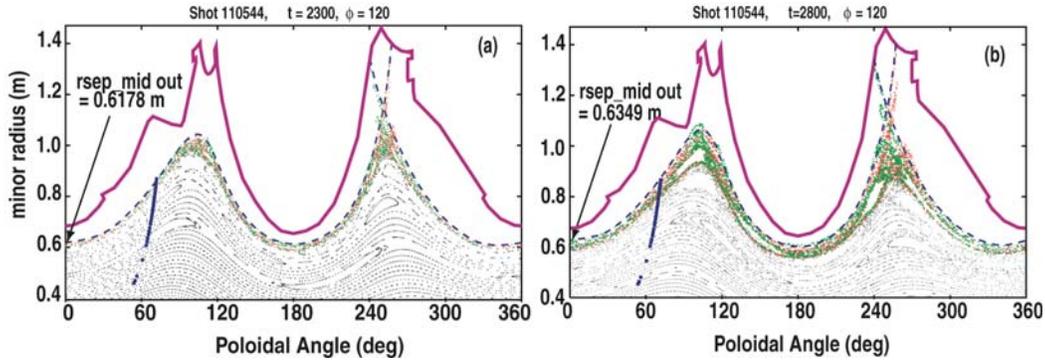
Fig. 4. TRIP3D results for DIII-D discharge 110544 at (a) 2300 ms and (b) 2800 ms. Black dots represent field lines that do not cross the unperturbed separatrix. Red and green dots represent field lines integrated in the forward (red) and reverse (green) $B_T$ direction that intersect a material surface.

The structure of the field lines near the lower divertor x-point indicates that, in addition to those field lines lost very close to the unperturbed inner and outer divertor legs, there are secondary striations further away from the legs at 2800 ms that are not seen at 2300 ms. These secondary striations intersect the divertor about 100-135 mm away from the nominal strikepoints (both along the inner wall above the inner strikepoint and outside the outer strikepoint in the outer scrape-off layer) and indicate a significant broadening of the magnetic flux profiles on the divertor targets and thus a broadening of the heat and particle flux profiles. Comparison with stochastic boundary results from non-diverted tokamaks indicates that a significant difference in diverted tokamaks is a "focusing" of the magnetic field line loss into the vicinity of the divertor. The complex structure of the stochastic layer can also be seen in the profile of the parallel connection length $L_c$ of the magnetic field lines to material surfaces (Fig. 5). $L_c$ generally increases as one moves into the plasma core, but there is significant structure. For comparison, the parallel connection length to the divertor target for field lines just outside the separatrix in the unperturbed equilibrium is about 50 m, while the collisional mean free path varies from 16 m to 62 m across the stochastic layer.
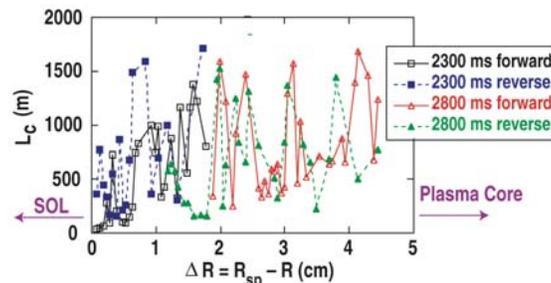


Fig. 5. Field line connection length from outboard midplane ($\phi = 120°$) to the vessel wall at 2300 ms (squares) and 2800 ms (triangles). Open symbols correspond to the connection length in the forward $B_T$ direction; solid symbols correspond to the reverse $B_T$ direction.

## V. PLASMA RESPONSE AND COMPATIBILITY WITH HIGH PERFORMANCE

Previous experimental studies of stochastic boundaries in ohmically heated, circular, limiter tokamaks have shown a $T_e$ profile flattening across the stochastic region (Fig. 6) which substantially increases $\nabla T_e$ deeper inside the plasma [7]. Similar profile flattening has been seen in "quiescent double barrier" (QDB) discharges, an ELM-free H–mode regime in the DIII–D tokamak [14]. A 3 cm flat region in $T_e$ [Fig. 7(b)] and a corresponding 4 cm flat region in the plasma density [Fig. 7(a)] are seen during the QDB phase of this discharge, a result that is typical of QDB discharges with a strong edge harmonic oscillation (EHO). Simulations of this discharge produce a 4 cm wide stochastic layer at the location of the Thomson scattering system used to measure the $T_e$ profile. The density profile flattening could result from the combination of an edge stochastic layer (model prediction) and the quiescent H–mode radial transport barrier (measured). While this flattening is consistent with the stochastic layer width modeled with TRIP3D, it has not been proven that these flat spots are caused by some combination of $\delta b_r$ due to the C–coil, error fields, or internal modes (such as the magnetic field of the EHO itself). Proof of an edge stochastic layer in a high performance QDB discharge would establish the compatibility of edge stochastic layers with high confinement. Alternatively, proof of the lack of a stochastic layer would establish the need to understand the nonlinear plasma response to stochastic layers. The limited experimental data available suggest that, for circular, limiter, ohmically heated discharges, vacuum magnetic field line integration results are a reasonable quantitative match to the plasma response [11]. This indicates that little plasma "self-healing" occurs under those conditions. In high performance DIII–D discharges, however, the power flow or momentum input from neutral beamheating might produce a plasma response which significantly heals the stochasticity via plasma rotation or some other effect. Understanding this nonlinear plasma response is critical for interpreting experimental results for tokamak pedestal and scrapeoff layer physics, and for developing predictive models of tokamak edge plasmas. Such understanding might, in turn, lead to new techniques for controlling the pedestal and boundary of high performance tokamaks.
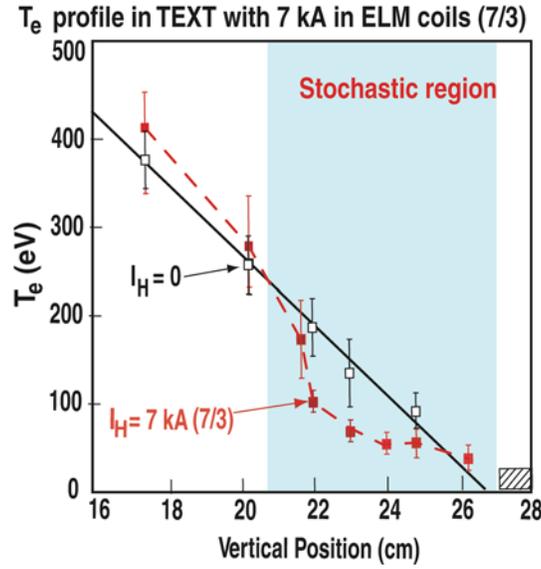
Fig. 6. H-mode-like $T_e$ gradient formed across the stochastic layer in the TEXT tokamak with 7 kA in the Ergodic Magnetic Limiter coils [7]. The steep gradient region forms at the inner edge of the stochastic region.
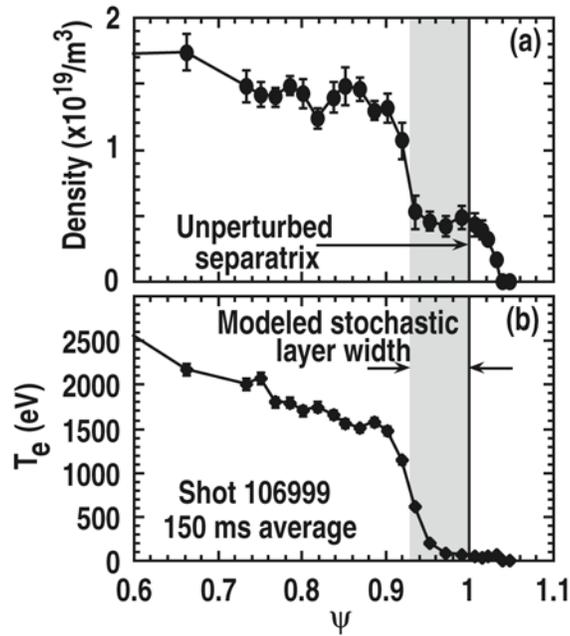


Fig. 7. Plasma density (a) and $T_e$ (b) profiles from Thomson scattering for QDB shot 106999 showing flat regions at the edge coincident with the stochastic layer width modelled with TRIP3D.

# REFERENCES

[1]     N. Pomphrey, A. Reiman, Phys. Fluids B **4**, 938 (1992).

[2]     T.E. Evans, *et al.* J. Nucl. Mater. **241**-**243**, 606 (1997).

[3]     R.J. La Haye, A.W. Hyatt, S.T. Scoville, Nucl. Fusion **32**, 2119 (1992).

[4]     T.E. Evans and the ASDEX Team, MPl-Garching Report IPP III/154, March, 1991.

[5]     T.E. Evans, *et al.*, J. Nucl. Mater. **220**-**222**, 235 (1995).

[6]     Ph. Gendrih, *et al.*, J. Nucl. Mater. **290**-**293**, 798 (2001).

[7]     T.E. Evans, *et al.*, J. Nucl. Mater. **145**-**146**, 812 (1986).

[8]     A.M. Garofalo, T.H. Jensen, L.C. Johnson et al., Phys. Plasmas **9**, 1997 (2002).

[9]     R.J. La Haye, *et al*. Phys. Plasmas **9**, 2051 (2002).

[10]    T.H. Osborne, *et al.*, Plasma Physics and Controlled Fusion, in press (2001).

[11]    T.E. Evans, R.A. Moyer, and P. Monat, "Modeling of stochastic magnetic flux loss from the edge of a poloidally diverted tokamak," GA-A23965, General Atomics, 2002; subm. to: Phys. Plasmas.

[12]    L. Lao, *et al.*, Nucl. Fusion **25**, 1611 (1985).

[13]    T.E. Evans and R.A. Moyer, "Modeling of coupled edge stochastic and core resonant magnetic field effects in diverted tokamaks," J. Nucl. Mater. in press (2002).

[14]    K.H. Burrell, *et al.*, Phys. Plasmas **8**, 2153 (2001).

# ACKNOWLEDGMENT